Int. J. Solids Structures Vol. 29, No. 11, pp. 1339–1350, 1992
Printed in Great Britain.

0020-7683/92 $5.00 + .00

THE GROWTH OF MICROVOIDS UNDER INTENSE DYNAMIC LOADING

RAUL CORTES
Department of Materials Science, E.T.S. Ingenieros de Caminos, Canales y Puertos, Polytechnic University of Madrid, Ciudad Universitaria, 28040 Madrid, Spain

(*Received* 29 *April* 1991; *in revised form* 16 *September* 1991)

Abstract—This paper deals with the analytical study of the dynamic growth of microvoids. A previous model by Carroll and Holt (1972), Static and dynamic pore-collapse relations for ductile porous materials, *J. Appl. Phys.* **43**, 1626–1636, for porous perfectly plastic materials under the action of a purely hydrostatic stress is further developed to include the influence of material viscosity, strain hardening and thermal softening in the tensile fracture behaviour. The results of this analysis are discussed with the help of a numerical study of the void growth relationships derived; the conclusion is that both material viscosity and strain hardening may have an important influence on the tensile strength of ductile materials at high strain rates. It is also shown that, in the conditions of the analysis, thermal softening by itself has a negligible influence on the dynamic tensile strength at high strain rates due to excessively localized heat generation near the surface of the voids.

1. INTRODUCTION

High tensile stresses may develop within a material as a result of the interaction of stress waves, and dynamic failure in the form of an internal cavitation may take place. This type of failure, termed spall fracture, may be either brittle or ductile. Brittle spall is controlled by the evolution of *microcracks* in the material which propagate and finally coalesce to generate the spall plane. The fracture may eventually be accompanied by a considerable plastic deformation around the microcracks. On the other hand, ductile spall is controlled by the dynamic evolution and coalescence of *microvoids*, accompanied by a large plastic deformation of the material around the voids.

The evolution of material response during spall is a complex problem. It is recognized that the presence of pre-existing heterogeneities can lead to the opening of cracks or voids and the initiation of the spall process. Experimental evidence suggests that there exists a threshold tensile stress at which spall initiation takes place. However, a material can bear tensile stresses considerably larger than such threshold stress without causing an important fracture process. This is due to the inertia and the kinetics associated with the micromechanisms controlling the spall type of fracture.

Several attempts have been made to define the phenomena controlling spall fracture. It has been established that spall fracture is associated with the complicated concurrence of nucleation, growth and coalescence of microdefects, which can depend on both the pre-existing and the evolving microstructure. Based on experimental arrangements, such as that of plate to plate impact, the detailed damage processes associated with spall have been carefully studied, and statistical laws for the nucleation and growth of microcracks or microvoids under given experimental conditions have been proposed. This latter approach needs the experimental determination of several parameters, which is rather complicated in practice. Review articles by Curran (1982), Curran *et al.* (1987) and Meyers and Aimone (1983), explain in some detail the most relevant results of both experimental and theoretical studies of spall fracture.

In the present paper we are concerned with the *ductile type* of spall fracture and our approach differs from those mentioned above. In particular, we analyse in detail the plastic void growth process which takes place under extremely high rates of loading. The basic assumptions of this analysis are taken from a previous model for perfectly plastic porous materials presented by Carroll and Holt (1972) for shrinking pores, and later extended by Johnson (1981) to pore expansion. The voids are assumed to be spherical and to grow plastically under the action of an externally applied macroscopic hydrostatic stress. The

influence of material viscosity, strain hardening and thermal softening effects on the dynamic void growth equation are ascertained. One of the advantages of using an analytical approach is that the influence of different effects on the dynamic void growth can be isolated and studied in greater depth. The influence of triaxiality in the void growth process is not considered, since in the light of the works by Gurson (1977), Rice and Tracey (1969), Cocks (1989) and others on static void growth, it becomes clear that the inclusion of triaxiality in the void expansion analysis greatly complicates the problem. So, numerical techniques are frequently employed when triaxiality effects are important (Tvergaard, 1982, Koplik and Needleman, 1988, Becker *et al.*, 1989). Moreover, it is expected that under extremely high loading rates, the hydrostatic stress will be the leading stress component in the spall fracture process.

2. RELATIONS FOR DYNAMIC VOID GROWTH UNDER HYDROSTATIC STRESSES

2.1. *General equation*

As a first step, a general relationship is derived between external hydrostatic stress and material porosity. Such a relation allows us to discuss within the same reference frame the growth of cavities when different yield criteria are considered. In the following sections, the influence of strain-rate, plastic strain and temperature on yield strength are analysed.

Starting with the simple assumptions of Carroll and Holt (1972), a uniform and homogeneous distribution of spherical voids is assumed. The process of hole growth can be modelled following the evolution of a hollow sphere of inner radius a (a_0, initial void radius) and external radius b (radius of the zone of influence of each pore), subjected to external stress σ, as shown in Fig. 1. Furthermore, the material is considered incompressible.

The relevant dynamic equilibrium equation for the model is:

$$\frac{\partial \sigma_r}{\partial r} + 2\frac{\sigma_r - \sigma_\theta}{r} = \rho \frac{d^2 r}{dt^2} \tag{1}$$

where σ_r is the radial stress, σ_θ the hoop stress and ρ the material density, r is an inner radius between a and b, and t is time. On integrating this equation, and after some manipulation, the following expression for the dynamic growth of cavities under an external stress σ at every instant t, is obtained (Carroll and Holt, 1972, Johnson, 1981):

$$\sigma + 2\int_1^{b/a} \frac{\Delta}{R}\, dR = \frac{\rho a_0^2}{3(\alpha_0 - 1)^{2/3}} Q(\ddot{\alpha}, \dot{\alpha}, \alpha) \tag{2}$$

where $\Delta = \sigma_r - \sigma_\theta$, $R = r/a$ and Q is given by:

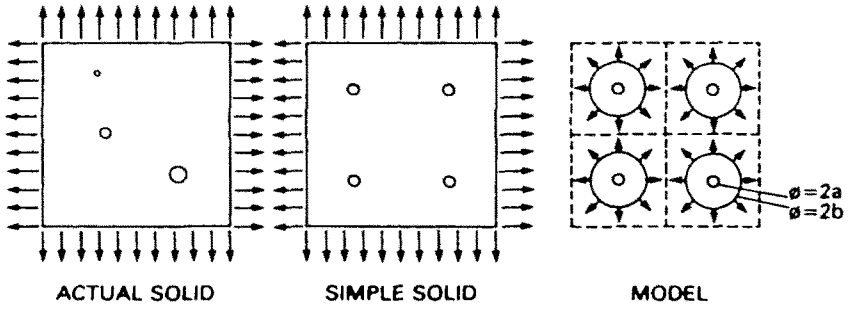

Fig. 1. Graphical representation of the simplifications of the model. To the left the actual solid with an irregular distribution of voids is shown. In the center, the actual void distribution is replaced by a distribution of single-sized equally separated voids. To the right, the radius of influence surrounding each void is shown.

$$Q(\ddot{\alpha}, \dot{\alpha}, \alpha) = \ddot{\alpha}[(\alpha-1)^{-1/3} - \alpha^{-1/3}] - \frac{\dot{\alpha}^2}{6}[(\alpha-1)^{-4/3} - \alpha^{-4/3}] \tag{3}$$

where dots indicate time differentiation and α, the distention factor of the material, is defined as:

$$\alpha = \frac{b^3}{b^3 - a^3}. \tag{4}$$

It has been previously determined that the period of the sphere deformation process while the material near the void is plastic and the farther material is still elastic is in practice sufficiently brief to be ignored, Johnson (1981), and, in consequence, we can reasonably assume that the hollow sphere will be at a fully plastic stage from the very beginning of the deformation process. Hence, for a growing void we will have:

$$\Delta = -\sigma_e \tag{5}$$

where the yield strength σ_e is determined by the particular constitutive equation of the material. For a perfectly plastic material, for instance, where σ_e equals a constant value σ_0, eqn (2) becomes:

$$\sigma - \frac{2\sigma_0}{3}\ln\left(\frac{\alpha}{\alpha-1}\right) = \frac{\rho a_0^2}{3(\alpha_0-1)^{2/3}} Q(\ddot{\alpha}, \dot{\alpha}, \alpha). \tag{6}$$

This expression was previously derived by Carroll and Holt (1972) for the case of shrinking pores.

2.2. *Strain rate dependence of the yield stress*

We now assume a dependence of the yield stress of the type:

$$\sigma_e = \sigma_0(1 + B\dot{\varepsilon}^m) \tag{7}$$

where the plastic strain rate $\dot{\varepsilon}$ is defined by $\dot{\varepsilon}^2 = 2\dot{\varepsilon}_{ij}\dot{\varepsilon}_{ij}/3$, the $\dot{\varepsilon}_{ij}$ being the components of the plastic strain rate tensor. Since we have a plastic deformation process with spherical symmetry, the equivalent plastic strain is given by Johnson and Mellor (1973):

$$\varepsilon = 2\ln\left(\frac{r}{r_0}\right) \tag{8}$$

and the corresponding strain rate is:

$$\dot{\varepsilon} = 2\frac{\dot{r}}{r}. \tag{9}$$

Taking into account material incompressibility:

$$r^3 = r_0^3 + a_0^3\frac{\alpha - \alpha_0}{\alpha_0 - 1} \tag{10}$$

and noting from the above expression that $a^3(\alpha_0 - 1) = a_0^3(\alpha - 1)$, we finally get:

$$\dot{\varepsilon} = \frac{2}{3(\alpha-1)}\frac{\dot{\alpha}}{R^3} \tag{11}$$

and from (2), (5) and (7), one obtains the following relation for hole growth under hydrostatic stress σ:

$$\sigma - \frac{2\sigma_0}{3}\ln\left(\frac{\alpha}{\alpha-1}\right) - \frac{2\sigma_0 B}{3m}(2\dot{\alpha}/(3(\alpha-1)))^m(1-((\alpha-1)/\alpha)^m) = \frac{\rho a_0^2}{3(\alpha_0-1)^{2/3}}Q(\ddot{\alpha},\dot{\alpha},\alpha). \tag{12}$$

Alternatively, if we assume a dependence of the yield stress of the type:

$$\sigma_e = \sigma_0\left\{1+\beta\ln\left(\frac{\dot{\varepsilon}}{\dot{\varepsilon}_0}\right)\right\} \tag{13}$$

then the dynamic void growth equation (2) becomes:

$$\sigma - \frac{2\sigma_0}{3}\ln\left(\frac{\alpha}{\alpha-1}\right) - \frac{2\sigma_0\beta}{3}\ln\left(\frac{2\dot{\alpha}}{3(\alpha-1)\dot{\varepsilon}_0}\right)\ln\left(\frac{\alpha}{\alpha-1}\right) + \frac{\beta\sigma_0}{3}[\ln(\alpha/(\alpha-1))]^2 = \frac{\rho a_0^2}{3(\alpha_0-1)^{2/3}}Q(\ddot{\alpha},\dot{\alpha},\alpha). \tag{14}$$

2.3. *Strain hardening dependence of the yield stress*

Strain hardening can be accounted for by means of a simple equation of the type:

$$\sigma_e = \sigma_0(1+H\varepsilon). \tag{15}$$

From eqn (8) and material incompressibility one can deduce that

$$\varepsilon = -\tfrac{3}{2}\ln\left(1-\frac{\alpha-\alpha_0}{(\alpha-1)R^3}\right) \tag{16}$$

and since

$$\ln(1-x) = -\sum_1^\infty \frac{x^n}{n} \tag{17}$$

then eqn (2) for hole growth becomes

$$\sigma - \frac{2\sigma_0}{3}\ln\left(\frac{\alpha}{\alpha-1}\right) - \frac{4\sigma_0}{9}HF_1(\alpha,\alpha_0) = \frac{\rho a_0^2}{3(\alpha_0-1)^{2/3}}Q(\ddot{\alpha},\dot{\alpha},\alpha) \tag{18}$$

where

$$F_1(\alpha,\alpha_0) = \sum_1^\infty \frac{(\alpha-\alpha_0)^n}{(\alpha-1)^n n^2}(1-((\alpha-1)/\alpha)^n). \tag{19}$$

2.4. *Strain rate and strain hardening dependence of the yield stress*

In a manner similar to that of the previous sub-sections, if the yield stress is represented by

$$\sigma_e = \sigma_0(1+H\varepsilon)(1+B\dot{\varepsilon}^m) \tag{20}$$

it can be easily verified that the differential equation for the dynamic void growth is given by

$$\sigma - \frac{2\sigma_0}{3}\ln\left(\frac{\alpha}{\alpha-1}\right) - \frac{4\sigma_0}{9}HF_1(\alpha,\alpha_0) - \frac{2\sigma_0 B}{3m}(2\dot{\alpha}/(3(\alpha-1)))^m(1-((\alpha-1)/\alpha)^m)$$
$$- \frac{2\sigma_0 BH}{3}(2\dot{\alpha}/(3(\alpha-1)))^m F_2(\alpha,\alpha_0) = \frac{\rho a_0^2}{3(\alpha_0-1)^{2/3}}Q(\ddot{\alpha},\dot{\alpha},\alpha) \tag{21}$$

where

$$F_2(\alpha,\alpha_0) = \sum_1^c \frac{(\alpha-\alpha_0)^n}{(\alpha-1)^n n(n+m)}(1-((\alpha-1)/\alpha)^n). \tag{22}$$

On the other hand, if we consider a yield stress dependence of the type:

$$\sigma_e = \sigma_0(1+H\varepsilon)\left[1+\beta\ln\left(\frac{\dot{\varepsilon}}{\dot{\varepsilon}_0}\right)\right] \tag{23}$$

we find that the dynamic pore growth process is governed by the equation

$$\sigma - \frac{2\sigma_0}{3}\ln\left(\frac{\alpha}{\alpha-1}\right) - \frac{2\sigma_0\beta}{3}\ln\left(\frac{2\dot{\alpha}}{3(\alpha-1)\dot{\varepsilon}_0}\right)\ln\left(\frac{\alpha}{\alpha-1}\right) + \frac{\beta\sigma_0}{3}[\ln(\alpha/(\alpha-1))]^2 - \frac{4\sigma_0}{9}HF_1(\alpha,\alpha_0)$$
$$- \frac{4\sigma_0\beta H}{9}\ln\left(\frac{2\dot{\alpha}}{3(\alpha-1)\dot{\varepsilon}_0}\right)F_1(\alpha,\alpha_0) + \frac{4\sigma_0\beta H}{9}F_3(\alpha,\alpha_0) = \frac{\rho a_0^2}{3(\alpha_0-1)^{2/3}}Q(\ddot{\alpha},\dot{\alpha},\alpha) \tag{24}$$

where

$$F_3(\alpha,\alpha_0) = \sum_1^c \frac{(\alpha-\alpha_0)^n}{(\alpha-1)^n n}\left[\frac{1-((\alpha-1)/\alpha)^n}{n^2} - \frac{((\alpha-1)/\alpha)^n\ln(\alpha/(\alpha-1))}{n}\right]. \tag{25}$$

2.5. *Temperature dependence of the yield stress with or without simultaneous strain hardening*

An aspect worth considering in the dynamic growth of voids under external stress is the temperature increase in the material as the result of the plastic work dissipated as heat. For materials experiencing linear thermal softening, the yield stress dependence may be written as

$$\sigma_e = \sigma_0\left(1-\frac{T}{\theta}\right) \tag{26}$$

where T is temperature and θ can be roughly identified with the melting temperature, both measured with respect to a reference value. It is worth noting that in this situation the plastic deformation is unstable and may give rise eventually to plastic strain localization in the presence of perturbations, Bai (1982). However, this case retains its interest because there is a delay between the instant of reaching the instability condition and that when strain localization is achieved, Grady and Kipp (1987). Under extremely high strain rate loading, this delay may be an important fraction of the total loading time, or even longer. Furthermore, in doing so we can isolate the thermal softening effect from other factors and so study it in greater depth.

We now consider the case of a non-conducting material. In this case, we can estimate the local temperature increment from the expression:

$$dT = \frac{\kappa\sigma_0}{\rho C}\left(1 - \frac{T}{\theta}\right) d\varepsilon \tag{27}$$

where C is the specific heat and κ is the coefficient of Taylor and Quinney (1934), a value of about 0.9 for metals. On integrating this latter equation from the initial state, we obtain

$$\left(1 - \frac{T}{\theta}\right) = (r_0/r)^{3\lambda} \tag{28}$$

where

$$\lambda = \frac{2\kappa\sigma_0}{3\rho C\theta}. \tag{29}$$

Since

$$(1-x)^\lambda = 1 + \sum_1^\infty (-1)^n \lambda(\lambda-1)\ldots(\lambda-n+1)\frac{x^n}{n!} \tag{30}$$

we can write

$$\left(1 - \frac{T}{\theta}\right) = 1 + \sum_1^\infty (-1)^n \frac{(\alpha-\alpha_0)^n}{(\alpha-1)^n} \lambda(\lambda-1)\ldots(\lambda-n+1)\frac{1}{n!\,R^{1n}} \tag{31}$$

where eqns (10) and (28) are taken into account, and finally the differential equation governing the dynamic pore growth problem comes to be

$$\sigma - \frac{2\sigma_0}{3}\ln\left(\frac{\alpha}{\alpha-1}\right) - \frac{2\sigma_0}{3}F_4(\alpha,\alpha_0) = \frac{\rho a_0^2}{3(\alpha_0-1)^{2/3}}Q(\ddot{\alpha},\dot{\alpha},\alpha) \tag{32}$$

where

$$F_4(\alpha,\alpha_0) = \sum_1^\infty (-1)^n \lambda(\lambda-1)\ldots(\lambda-n+1)\frac{1}{n!\,n}\left\{\frac{(\alpha-\alpha_0)^n}{(\alpha-1)^n}(1-((\alpha-1)/\alpha)^n)\right\}. \tag{33}$$

Now, consider yielding which exhibits simultaneously strain hardening and thermal softening, of the type

$$\sigma_e = \sigma_0(1+H\varepsilon)\left(1 - \frac{T}{\theta}\right). \tag{34}$$

For a non-conducting material the temperature increase is obtained from the equation

$$\int_0^T \frac{dT}{(1-T/\theta)} = \int_0^\varepsilon \frac{\kappa\sigma_0}{\rho C}(1+H\varepsilon)\,d\varepsilon \tag{35}$$

or

$$\left(1 - \frac{T}{\theta}\right) = (r_0/r)^{3\lambda(1-H\ln(r_0/r))} \tag{36}$$

and the yielding equation (34) can be written as a function of R, as shown in the Appendix, as:

$$\sigma_e = \sigma_0\left(1+\sum_{n=1}^{\infty} D_n \frac{1}{R^{3n}} + \sum_{p=1}^{\infty}\sum_{q=1}^{\infty} E_{pq} \frac{1}{R^{3(p+q)}} + \sum_{p=1}^{\infty}\sum_{q=1}^{\infty}\sum_{r=1}^{\infty} G_{pqr} \frac{1}{R^{3(p+q+r)}}\right). \quad (37)$$

Using this expression, the governing equation of the dynamic void growth process becomes

$$\sigma - \frac{2\sigma_0}{3}\ln\left(\frac{\alpha}{\alpha-1}\right) - \frac{2\sigma_0}{3} F_5(\alpha,\alpha_0) = \frac{\rho a_0^2}{3(\alpha_0-1)^{2/3}} Q(\ddot{\alpha},\dot{\alpha},\alpha) \quad (38)$$

where

$$F_5(\alpha,\alpha_0) = \sum_{n=1}^{\infty} D_n \frac{1-\xi^n}{n} + \sum_{p=1}^{\infty}\sum_{q=1}^{\infty} E_{pq} \frac{1-\xi^{(p+q)}}{p+q} + \sum_{p=1}^{\infty}\sum_{q=1}^{\infty}\sum_{r=1}^{\infty} G_{pqr} \frac{1-\xi^{(p+q+r)}}{p+q+r}. \quad (39)$$

In the above expression, ξ is the material porosity defined as $\xi = (a/b)^3$. We remark that ξ is related to the distention factor α by the expression $\xi = (\alpha-1)/\alpha$.

Finally, if a yield stress dependence of the type

$$\sigma_e = \sigma_0(1+H\varepsilon)\left(1+\beta\ln\left(\frac{\dot{\varepsilon}}{\dot{\varepsilon}_0}\right)\right)\left(1-\frac{T}{\theta}\right) \quad (40)$$

is assumed, then the solution of the coupled thermo-mechanical problem depends on the loading history and has to be solved by numerical methods.

3. NUMERICAL ANALYSIS

In this section, we analyse numerically the analytical formulation previously developed, assuming a material subjected to a linearly increasing hydrostatic stress and determining the influence of the different yielding functions on dynamic pore growth. So, we consider now the influence of a viscous term, the strain hardening and the thermal softening effects.

For this analysis we have chosen the parameters $\sigma_0 = 200$ MPa, $C = 902$ J kg^{-1} K^{-1} and $\rho = 2700$ kg m^{-3}, which may correspond to an aluminium. Some simulations for a copper-like material, with $\sigma_0 = 150$ MPa, $C = 385$ J kg^{-1} K^{-1} and $\rho = 8930$ kg m^{-3}, were also performed. A value of $a_0 = 10^{-6}$ m for the initial pore size was selected, as well as an initial porosity of $\xi_0 = 10^{-4}$, where porosity is defined as $\xi = (\alpha-1)/\alpha$. Unless otherwise indicated, a hydrostatic loading pulse increasing at a constant rate of 10 GPa μs^{-1} was assumed.

The evolution of porosity with time was obtained from the numerical integration of the corresponding dynamic void growth equation. It is well known that coalescence of cavities takes place at a given instant as voids grow. In this simulation, and just to fix ideas, it is assumed that coalescence takes place by direct impingement of the cavities when the distance between cavities equals the void radius. This implies that the corresponding porosity at the instant of coalescence equals $\xi = 0.30$. In consequence the dynamic tensile strength is defined as the hydrostatic stress acting on the material for a porosity value of $\xi = 0.30$. So the numerical analyses are made up to the moment when a value of $\xi = 0.30$ is reached. The selection of this critical porosity value agrees with experimental measurements of void volume fraction at the fracture plane in spall experiments performed in copper, Johnson (1981). Moreover, Grady (1988) has suggested for ductile fracture that coalescence might begin for a void volume fraction of the same order of magnitude of that here selected.

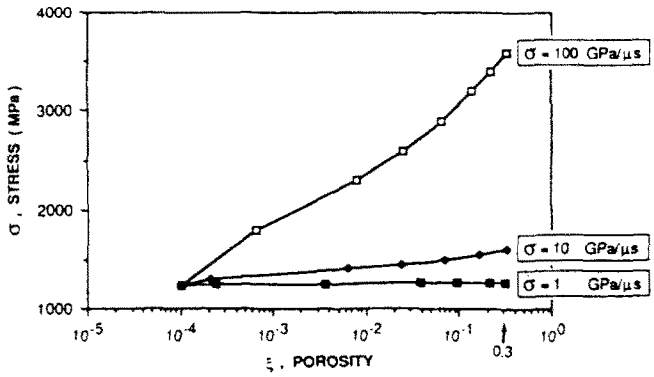

Fig. 2. Dynamic porosity growth curves for a perfectly plastic aluminium-like material.

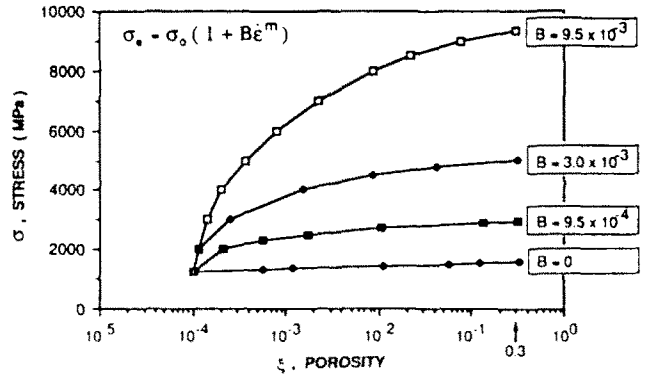

Fig. 3. Influence of viscosity in the dynamic growth of cavities.

Figure 2 presents the stress–porosity curves for a perfectly plastic behaviour of the aluminium-like material subjected to loading rates of 1.0 GPa μs^{-1}, 10 GPa μs^{-1} and 100 GPa μs^{-1}.

Figure 3 is for the case of the aluminium-like material with the viscous resistance term given by eqn (7) with $m = 0.5$ and for different values of parameter B. Parameter B was estimated as $B = D/\dot{\varepsilon}_0^m$, with $D = 3.0$ and $\dot{\varepsilon}_0 = 10^5\ s^{-1}$, $10^6\ s^{-1}$ and $10^7\ s^{-1}$ alternatively, giving different degrees of strain rate sensitivity in the high strain rate range ($\dot{\varepsilon} > 10^4\ s^{-1}$). This figure shows that the strain rate sensitivity of materials in the high strain rate range has a remarkable influence on the tensile strength of the material.

The influence of strain hardening on dynamic void growth is illustrated in Fig. 4; Fig. 4a shows the results obtained for the aluminium-like material, where a hardening parameter $H = 1$ was chosen, whereas Fig. 4b shows the results for the copper-like material, where values of $H = 5.0$ and $H = 10.0$ were taken.

Figure 5 illustrates the influence of thermal softening on the porosity curves for the aluminum-like material by taking $\theta = 800$ K and $\kappa = 0.9$. Qualitatively similar results were obtained for copper.

4. DISCUSSION

Material viscosity, especially in the high strain-rate range, has a great influence on the dynamic tensile strength of aluminium as shown in the previous section. This is a useful result since the practical determination of material properties at such high strain rates is not an easy task. Strain hardening also has an important influence though less marked than the previous one. In particular, for aluminium it has an effect which can be disregarded in practice, whereas for greater amounts of work hardening, such as that exhibited by copper, the degree of influence on the dynamic tensile strength is greater.

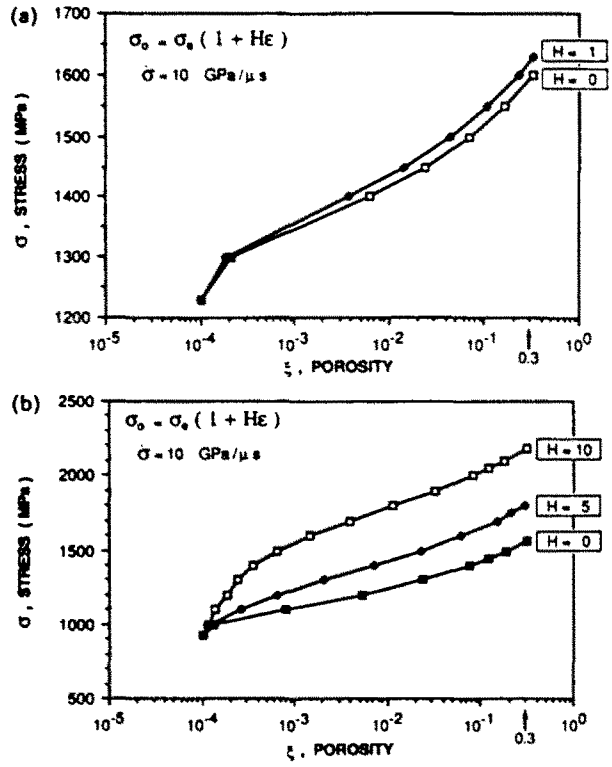

Fig. 4. (a) Influence of strain hardening in the dynamic growth of porosity for the aluminium-like material. (b) Influence of strain hardening in the dynamic growth of porosity for the copper-like material.

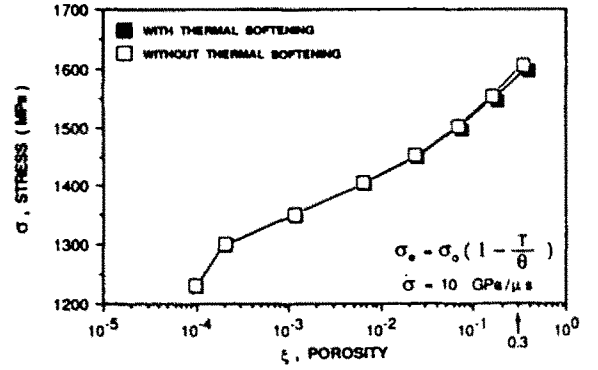

Fig. 5. Influence of thermal softening in the case of the aluminium-like material.

Thermal softening by itself has a negligible effect on tensile strength under high loading rates, for both copper and aluminium. This result is based on the assumption of a vanishing value of thermal conductivity, but it is unlikely that the consideration of a finite conductivity modifies this conclusion. The average temperature increase within the zone of influence of a spherical cavity for a non-conducting material is given by, Cortés (1989):

$$\frac{\langle T \rangle}{\theta} = \frac{1}{1-\xi} \sum_{1}^{\infty} (-1)^{n+1} \frac{(\alpha-\alpha_0)^n}{(\alpha-1)^n} \frac{\lambda(\lambda-1)\ldots(\lambda-n+1)}{n!} c_n \tag{41}$$

where

$$c_1 = \xi \ln (1/\xi)$$

$$c_n = \frac{\xi - \xi^n}{n-1}, \quad (n > 1). \tag{42}$$

On the other hand, it is easy to verify that for a material with infinite thermal conductivity the corresponding temperature increase will be (Cortés, 1989)

$$\frac{T}{\theta} = 1 - \frac{(\alpha_0 - 1)^4}{(\alpha - 1)^4} \frac{\xi^{2(1-\xi)}}{\xi_0^{2(1-\xi_0)}}. \tag{43}$$

For an initial porosity of $\xi_0 = 10^{-4}$ and a final porosity of $\xi = 0.1$, eqn (41) gives an average temperature increase of only 1.64% of the melting temperature of aluminium, and about 0.70% of the melting temperature for copper. These results reflect the limited influence of the thermal softening effect on the dynamic growth of microvoids. Moreover, for aluminium, for instance, and for a porosity value of $\xi = 0.1$, it can be shown that the temperature in the inner wall of the void ($r = a$) will be about the melting temperature; at $r = 1.05a$, the temperature increase will be about only 12% of the melting temperature, whereas at $r = b = 2.15a$, the temperature increase is less than about 1% of the melting temperature. Consequently, although the temperature increase in the inner wall of the cavity may be a substantial fraction of the melting temperature of the material as previously noted by Johnson (1981), such an effect is so localized that it has a negligible influence on the global strength of the material. In fact, the geometric softening term $2\sigma_0/3 \ln(1/\xi)$ has a much more pronounced softening effect than the thermal effect. On the other hand, for $\xi_0 = 10^{-4}$ and $\xi = 0.1$, eqn (43) gives a temperature increase under the assumption of infinite thermal conductivity of about 2.19% of the melting temperature for aluminium and 0.94% for copper. So it is unlikely that the consideration of thermal conductivity effects in the analysis modifies the above conclusion.

5. CONCLUSIONS

(1) A model for dynamic growth of microvoids under hydrostatic stress, based on a previous one introduced by Carroll and Holt (1972) for shrinking pores, was extended to take into account the effect of material viscosity, strain hardening and thermal softening in the tensile fracture behaviour of ductile materials.
(2) Thermal softening by itself was found to have a negligible influence on dynamic tensile strength in the case of aluminium and copper-like materials, due to an excessively localized heat generation near the surface of the voids.
(3) Explicit expressions which allow to quantify the effects of material rate dependence in the high strain rate range (of the power law and logarithmic types) and linear strain hardening in the dynamic growth of microvoids have been presented. Such factors may have an important effect on the dynamic growth of microvoids as reflected in the values of dynamic tensile strengths.

REFERENCES

Bai, Y. L. (1982). Thermoplastic instability in simple shear. *J. Mech. Phys. Solids* **30**, 195–207.
Becker, R., Smelser, R. E. and Richmond, O. (1989). The effect of void shape on the development of damage and fracture in plane-strain tension. *J. Mech. Phys. Solids* **37**, 111–129.
Carroll, M. M. and Holt, A. C. (1972). Static and dynamic pore-collapse relations for ductile porous materials. *J. Appl. Phys.* **43**, 1626–1636.
Cocks, A. C. F. (1989). Inelastic deformation of porous materials. *J. Mech. Phys. Solids* **37**, 693–715.
Cortés, R. (1989). Fracture and mechanical behaviour modelling of metallic materials at high strain rates. Ph.D. Thesis, Polytechnic University of Madrid.
Curran, D. R. (1982). Dynamic fracture. In *Impact Dynamics* (Edited by J. A. Zukas, T. Nicholas, H. F. Swift, L. B. Greszczuk and D. R. Curran). John Wiley & Sons, New York.
Curran, D. R., Seaman, L. and Shockey, D. A. (1987). Dynamic failure of solids. *Physics Rep.* **147**, 254–388.
Grady, D. E. (1988). The spall strength of condensed matter. *J. Mech. Phys. Solids* **36**, 353–384.
Grady, D. E. and Kipp, M. E. (1987). The growth of unstable thermoplastic shear with application to steady-wave shock compression in solids. *J. Mech. Phys. Solids* **35**, 95–118.
Gurson, A. L. (1977). Continuum theory of ductile rupture by void nucleation and growth: Part I—Yield criteria and flow rules for porous ductile media. *J. Engng Mater. Technol.* **99**, 2–15.
Johnson, J. N. (1981). Dynamic fracture and spallation in ductile solids. *J. Appl. Phys.* **52**, 2812–2825.
Johnson, W. and Mellor, P. B. (1973). *Engineering Plasticity*. Van Nostrand Reinhold, London.

Koplik, J. and Needleman, A. (1988). Void growth and coalescence in porous plastic solids. *Int. J. Solids Structures* **24**, 835–853.
Meyers, M. A. and Aimone, C. T. (1983). Dynamic fracture (spalling) of metals. *Prog. Mater. Sci.* **28**, 1–99.
Rice, J. R. and Tracey, D. M. (1969). On the ductile enlargement of voids in triaxial stress fields. *J. Mech. Phys. Solids* **17**, 201–217.
Taylor, G. J. and Quinney, H. (1934). The latent energy remaining in a metal after cold working. *Proc. R. Soc. London* **143A**, 307–326.
Tvergaard, V. (1982). On localization in ductile materials containing spherical voids. *Int. J. Fracture* **18**, 237–252.

APPENDIX

Equation (36) can also be expressed as:

$$\left(1-\frac{T}{\theta}\right)=S^{\alpha(1-H^{*}\ln(S))} \tag{A1}$$

where

$$S=(r_0/r)^3=1-\frac{\alpha-\alpha_0}{(\alpha-1)R^3}. \tag{A2}$$

After series expansion of the linear hardening term appearing in eqn (34), we can write

$$1+H\varepsilon=1+\frac{2H}{3}\sum_{1}^{\infty}\frac{(\alpha-\alpha_0)^n}{(\alpha-1)^n}\frac{1}{nR^{3n}}. \tag{A3}$$

The thermal softening term of eqn (34) can be expressed, through eqns (A1) and (A2), as the product of the following two series:

$$S^{\alpha}=1+\sum_{1}^{\infty}(-1)^n\lambda(\lambda-1)\ldots(\lambda-n+1)\frac{(\alpha-\alpha_0)^n}{(\alpha-1)^n n!\,R^{3n}} \tag{A4}$$

and

$$S^{\alpha H^{*}\ln(S)}=1+\sum_{1}^{\infty}a_n\frac{(\alpha-\alpha_0)^n}{(\alpha-1)^n n!\,R^{3n}}. \tag{A5}$$

In this latter equation, the a_n correspond to the nth derivatives of the left-hand-side computed for $x=((\alpha-\alpha_0)/(\alpha-1))/R^3=0$. Defining $f_1(x)$ as the left-hand-side of eqn (A5), and $h(x)$ as

$$h(x)=-\frac{\lambda H}{3}[\ln(1-x)]^2 \tag{A6}$$

it becomes clear that

$$f_1(x)=e^{h(x)}. \tag{A7}$$

Then, by successive derivation, we deduce that

$$\begin{aligned}
f_1' &= f_2 = f_1h_1\\
f_2' &= f_3 = f_1h_2+f_2h_1\\
f_3' &= f_4 = f_1h_3+f_2h_2+h_2f_2+f_1h_1\\
&\cdots\cdots\cdots\cdots\cdots\cdots\cdots\cdots\cdots\\
f_{n-1}' &= f_n = \sum_{0}^{n-2}f_{i+1}h_{n-i-1}\frac{(n-2)!}{i!\,(n-2-i)!}.
\end{aligned} \tag{A8}$$

In the above derivatives, h_k correspond to the kth derivative of function h, evaluated for $x=0$. Such derivatives may be evaluated in a recursive manner as

$$h_1=0,\quad h_{i+1}=ih_i-(i-1)!,\quad h_i=\frac{2\lambda h_i}{3}. \tag{A9}$$

Similarly, the f_k correspond to the $k-1$th derivative of function $f_1(x)$ computed at $x=0$, and since $a_{n-1}=f_n$, from the recursive manner expressed by eqns (A8), all of the required a_n can be calculated.

Finally, by defining:

$$A_n = \frac{2H}{3}\frac{(x-x_0)^n}{(x-1)^n n}$$

$$B_n = (-1)^n \lambda(\lambda-1)\ldots(\lambda-n+1)\frac{(x-x_0)^n}{(x-1)^n n!}$$

$$C_n = a_n \frac{(x-x_0)^n}{(x-1)^n n!} \tag{A10}$$

we can rewrite eqn (34) as

$$\sigma_e = \sigma_0 \left(1 + \sum_{n=1}^{\infty} D_n \frac{1}{R^{3n}} + \sum_{p=1}^{\infty}\sum_{q=1}^{\infty} E_{pq} \frac{1}{R^{3(p+q)}} + \sum_{p=1}^{\infty}\sum_{q=1}^{\infty}\sum_{r=1}^{\infty} G_{pqr} \frac{1}{R^{3(p+q+r)}}\right) \tag{A11}$$

where

$$D_n = A_n + B_n + C_n$$
$$E_{pq} = A_p B_q + B_p C_q + C_p A_q$$
$$G_{pqr} = A_p B_q C_r. \tag{A12}$$